RAPID COMMUNICATIONS

PHYSICAL REVIEW B VOLUME 49, NUMBER 19 15 MAY 1994-I

Band picture of the spin-Peierls transition in the spin-$\frac{1}{2}$ linear-chain cuprate $GeCuO_3$

L. F. Mattheiss
AT&T Bell Laboratories, Murray Hill, New Jersey 07974
(Received 15 October 1993)

The results of electronic-structure calculations for $GeCuO_3$ feature a pair of narrow ($\sim$ 1 eV) half-filled, one-dimensional σ^* conduction bands that originate from two edge-sharing CuO_2 linear chains in the orthorhombic cell. Unusual transport properties are predicted since the confined carrier motion along the chains (at any band filling) requires tunneling through nodal charge-density regions. At the spin-Peierls transition, the dimerization of the CuO_2 chains can open a band gap at E_F, provided that the Cu displacements in neighboring chains are staggered.

Recently, Hase, Terasaki, and Uchinokura[1] have identified $GeCuO_3$ as an inorganic compound that undergoes a spin-Peierls transition, a phenomenon that previously has been associated only with organic systems.[2] Specifically, Hase, Terasaki, and Uchinokura[1] have observed an abrupt decrease in the $GeCuO_3$ magnetic susceptibility near 14 K which they interpret as a phase transition from a uniform antiferromagnetic spin-$\frac{1}{2}$ Heisenberg chain to a system of dimerized chains with a singlet ground state and a $\sim$ 24-K energy gap. They argue that the magnetic-field dependence of the structural transition temperature confirms the spin-Peierls interpretation and excludes the possibility that an unrelated structural transition is involved. Subsequent studies have shown[3] that the $GeCuO_3$ spin-Peierls transition temperature is also reduced by Zn$\rightarrow$Cu doping, and the transition disappears entirely when the Zn-doping levels exceed 3%.

Single crystals of $GeCuO_3$ are translucent and blue in color.[1,4] Transport measurements[4] show that single-crystal samples exhibit insulating behavior, with room-temperature resistivities as high as $\rho_{300\ K} \approx 10^{13}\ \Omega$cm. However, ceramic samples that have been reduced in a H_2/N_2 atmosphere yield much lower ($\rho_{300\ K} \approx 30\ \Omega$cm) values and evidence for a modest ($\sim$ 0.02 eV) activation energy.[5] According to structural studies,[4,6] $GeCuO_3$ possesses an orthorhombic cell (see Fig. 1) that contains two vertex-linked CuO_6 octahedra which form edge-sharing

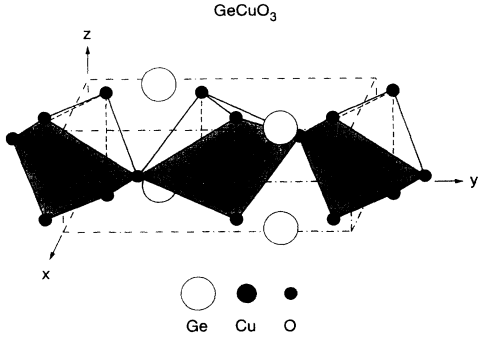

FIG. 1. Primitive orthorhombic cell for $GeCuO_3$ which features a pair of vertex-linked CuO_6 octahedra that share edges along c to form symmetry-related CuO_2 chains with Ge spacers.

CuO_2 chains along the c axis. These chains, which are uniform above the spin-Peierls transition, presumably become dimerized by the distortion near 14 K. However, the details of the low-temperature structure have not yet been determined. The present study predicts a specific model for the $GeCuO_3$ spin-Peierls distortion.

Although a spin-Peierls picture of the electrical and magnetic properties of $GeCuO_3$ implies that electron-correlation effects play an important role in determining the electronic properties of this material, it is nonetheless valuable to investigate the applicability of standard band methods and the local-density approximation[7] (LDA) to systems of this type. With this viewpoint in mind, a scalar-relativistic version[8] of the linear augmented-plane-wave (LAPW) method[9] has been applied in the present investigation to calculate the nonmagnetic band structure of orthorhombic $GeCuO_3$. Exchange and correlation effects have been included in the LDA with the use of the Wigner interpolation formula.[10]

The present LAPW implementation imposes no shape approximations. The LAPW basis has included plane waves with a 13.8-Ry cutoff ($\sim$ 350 LAPW's per formula unit) and spherical-harmonic terms through $l = 6$ inside the muffin-tin spheres. The charge density and potential are expanded in terms of $\sim$ 6000 plane waves (60 Ry) in the interstitial region and lattice-harmonic expansions ($l_{max} = 4$) within the muffin tins. A six-point $\mathbf{k}$ sample in the $\frac{1}{8}$ irreducible wedge has been used to perform Brillouin-zone (BZ) integrations. The atomic Ge($4s^24p^2$), Cu($3d^{10}4s^1$), and O($2s^22p^4$) states have been treated as valence electrons while a frozen-core approximation has been applied to the more tightly bound states.

As shown in Fig. 1, the room-temperature $GeCuO_3$ structure has orthorhombic symmetry [$Pbmm$ (D^5_{2h}) space group] and contains two formula units per primitive cell.[6] The structural results[6] show that the CuO_6 octahedra are stretched such that the Cu-O(1) bond distances [where O(1) labels the apical oxygens], d[Cu-O(1)]$\approx$ 2.77 Å, are significantly longer than the planar values, d[Cu-O(2)]$\approx$1.94 Å. Though less clearly depicted in Fig. 1, the Ge-O network also forms c-axis chains. Here, the Ge's are tetrahedrally coordinated by O's. The nearest-neighbor Ge-O bond lengths are unusually short [$\sim$ 1.77

and 1.72 Å for O(1) and O(2), respectively], and this is consistent with a formal Ge valence of 4+ in this material.

This expectation of a Ge^{4+} valence is confirmed by the LAPW results for $GeCuO_3$ which are plotted in Fig. 2. The 28-band valence manifold consists of 18 lower-lying O($2p$) states and ten Cu($3d$) bands near E_F. The lowest pair of unoccupied bands have predominant Ge($4s$) character. This feature is in sharp contrast to the corresponding results for another cuprate with a group-IVA constituent (i.e., Pb in $Pb_2Sr_2YCu_3O_8$) where the calculated[11] Pb($6s$) bands occur at energies $\sim$ 7–9 eV below E_F. However, the Pb^{2+} valence in $Pb_2Sr_2YCu_3O_8$ is consistent with the fact that the average Pb-O bond length ($\sim$ 2.6 Å) is larger than typical values ($\sim$ 2.2 Å in PbO_2) for Pb^{4+} compounds.

An eye-catching feature of the $GeCuO_3$ results in Fig. 2 is the presence of two nearly degenerate half-filled σ^* conduction bands with a surprisingly narrow ($\sim$ 1 eV) width. The fact that these σ^* bands are split-off in energy ($\sim$ 0.25 eV) from the fully occupied valence manifold suggests that an isostructural Ni compound (i.e., $GeNiO_3$) would be an ordinary semiconductor; however, efforts to synthesize this phase have been unsuccessful thus far.[12] These split-off σ^* bands contrast with the now familiar results[11] for typical cuprate high-T_c superconductors such as $Pb_2Sr_2YCu_3O_8$, where vertex-linked CuO_2 planes produce σ^* bands that overlap the valence-band complex in energy and exhibit overall bandwidths of $\sim$ 4 eV. As shown below, these differences have a simple geometric origin. In the high-T_c cuprates, the planar ($pd\sigma$) interactions provide a ($\sin\frac{1}{2}k_xa + \sin\frac{1}{2}k_ya$)-type dependence on wave vector,[13] vanishing at the zone-center Γ and reaching maxima at the BZ boundaries. Despite their visual simplicity, a tight-binding (TB) description of the $GeCuO_3$ σ^* bands is sufficiently complex to require a five-band model. The narrow width of this subband is due, not to weak bonding, but rather to a translation-induced switching between two sets of oxygen orbitals with comparable ($pd\sigma$) interactions.

A schematic representation of these effects is shown in Fig. 3. In a rotated coordinate system where x' is parallel to the edge-sharing O(2)'s in Fig. 1, the Cu($3d$) component of the σ^* band has $d(x'z)$ character. Since the CuO_6 octahedra share edges along z that are separated by the cell dimension c, translation symmetry imposes restrictions on the relative phases of the p-type orbitals at the upper and lower O(2) sites in Fig. 3. In the two-center approximation,[13] the dominant Cu-O(2) interaction involves nearly equal energy integrals ($E_{z,x'z} \approx E_{x',x'z}$) with ($\cos\frac{1}{2}k_zc$)- and ($\sin\frac{1}{2}k_zc$)-type factors, respectively. These combine to produce hybrid ($pd\sigma$) interactions that switch from $p(z)$ orbitals when $k_z = 0$ to $p(x')$ orbitals for $k_z = (\pi/c)$ with little change in strength, thereby yielding the narrow, molecular-orbital-type σ^* bands shown in Fig. 2.

According to this TB analysis, the individual $E_{z,x'z}$ and $E_{x',x'z}$ interactions depend on the geometric configuration of the O(2)-type oxygens that make up the base of the CuO_6 octahedra. For example, these interactions would be equal[13] if the arrangement of O(2) atoms that surround the central Cu site in Fig. 3 were square rather than rectangular (i.e., elongated along c). For this symmetric geometry, the σ^* bandwidth is reduced to zero, at least in the simplest TB treatment. In principle, one could even reverse the σ^* dispersion by increasing the O(2) separations along x' relative to those along z.

These orbital characteristics of the $GeCuO_3$ σ^* band are confirmed by the charge-density plots in the $x'z$ plane that are shown in Fig. 4. The left-hand panel illustrates the LAPW charge density in the σ^* bands, averaged over states in the $k_z = 0$ plane. The right-hand panel presents the corresponding $k_z = (\pi/c)$ results, where the effect of s-p hybridization is seen to enhance Cu-O(2) interactions along the chain and diminish interchain coupling. The contours for intermediate k_z's involve appropriate averages of these results. The antibonding character of the σ^* bands adds a novel aspect to these charge-density results in the form of nodes which are interspersed between neighboring sites along the chain. Intuitively, one expects that such nodes would inhibit charge transport along the chains, since itinerant carriers would have to

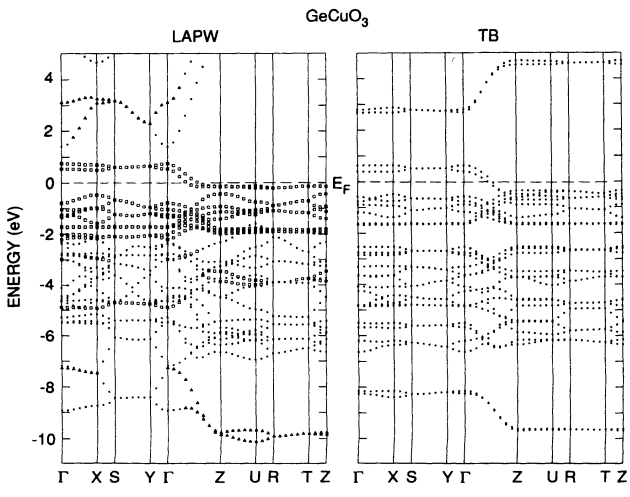

FIG. 2. LAPW and TB energy-band results for $GeCuO_3$ along several BZ directions ($\Gamma XSYT$ and $ZURTZ$) that are perpendicular and one (ΓZ) that is parallel to the linear-chain axes. LAPW bands with significant Cu($3d$) ($w_d > 0.3$) and Ge($4s4p$) ($w_{s,p} > 0.1$) orbital weight in the muffin tins are identified by squares and triangles, respectively.

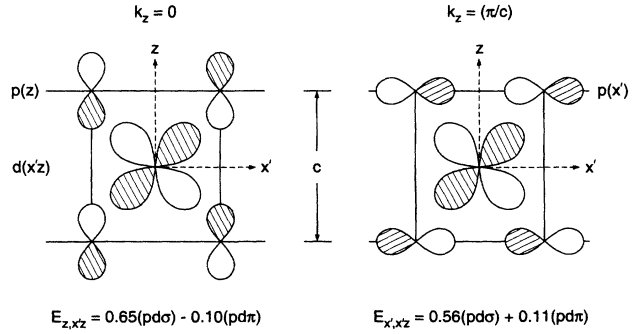

FIG. 3. Schematic representation of the five-band, two-component O($2p$)-Cu($3d$) interactions that produce the narrow molecular-orbital-type σ^* bands in $GeCuO_3$.

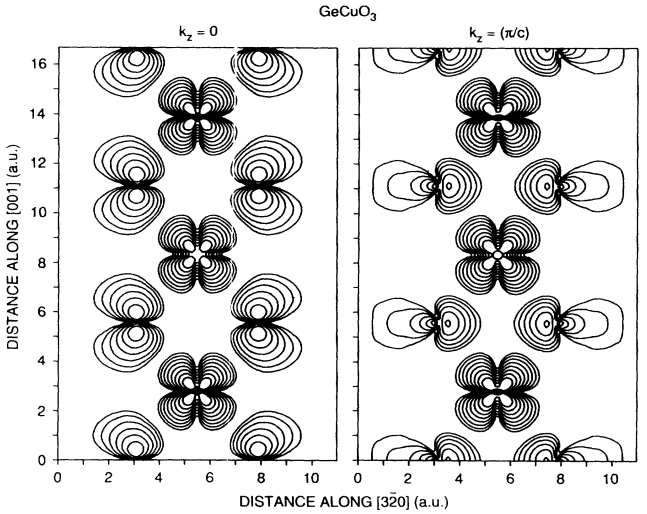

FIG. 4. Charge-density contours for the $GeCuO_3$ σ^* bands, averaged over wave vectors $\mathbf{k}$ in the central ($k_z = 0$) and top [$k_z = (\pi/c)$] BZ faces. The outermost contour values are 0.005 electrons/(a.u.)^3 and adjacent contours are doubled in magnitude.

tunnel through these low-density nodal regions. This could account for the extremely high room-temperature (RT) resistivities that are observed[4] in this system. In more typical two- or three-dimensional materials (including the high-T_c cuprates), analogous effects are diminished by the fact that such nodes are confined to *points* on the Fermi surface and alternative conduction paths (or bands) are available.

The $GeCuO_3$ density-of-states results, including projected contributions within the individual muffin-tin spheres, are shown in Fig. 5. The Ge component is relatively small over the energy range of the occupied valence band. Thus, like the Pb, Sr, and Y constituents[11]

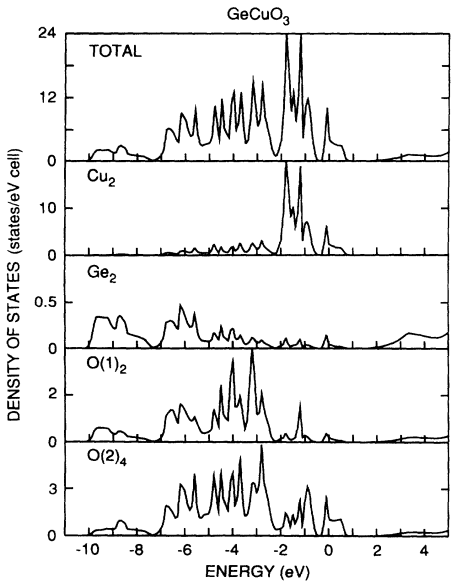

FIG. 5. Total and muffin-tin-projected density-of-states results for $GeCuO_3$.

TABLE I. Tight-binding parameters for $GeCuO_3$ (rms error ≈ 0.46 eV).

Sites	Distance (Å)	Parameters	Value (eV)
Ge		$\varepsilon_s, \varepsilon_p$	−1.02,5.0
Cu		ε_d	−1.80
O(1)		ε_p	−4.73
O(2)		ε_p	−2.65
Ge-O(1)	1.77	$(sp\sigma)$	3.21
		$(pp\sigma),(pp\pi)$	2.77,−1.53
Ge-O(2)	1.72	$(sp\sigma)$	2.91
		$(pp\sigma),(pp\pi)$	3.72,−1.41
Cu-O(1)	2.77	$(pd\sigma),(pd\pi)$	−0.44,0.17
Cu-O(2)	1.94	$(pd\sigma),(pd\pi)$	−1.39,0.61

of $Pb_2Sr_2YCu_3O_8$, Ge is an electronically inactive donor (i.e., Ge^{4+}) ingredient. This suggests that substitutional doping (Ga,As→Ge) at these sites should be explored as an alternative means for introducing carriers, since, in contrast to Zn→Cu substitutions,[3] the chain sites are less directly affected. The Cu($3d$) weight in Fig. 5 is localized within a narrow energy range near the Fermi level; this differs from results for typical high-T_c superconductors[11] where this weight is distributed uniformly over the entire valence band.

Details of the low-temperature structural distortion in $GeCuO_3$ are presently unavailable. To explore the effect of a few selected distortions on the $GeCuO_3$ bands near E_F, a 15-parameter TB model has been set up, based on a fit to LAPW results at eight BZ points (rms error ~ 0.5 eV). The resulting TB bands are plotted in the right-hand panel of Fig. 2 and the derived parameters are listed in Table I. Since the spin-Peierls distortion is ex-

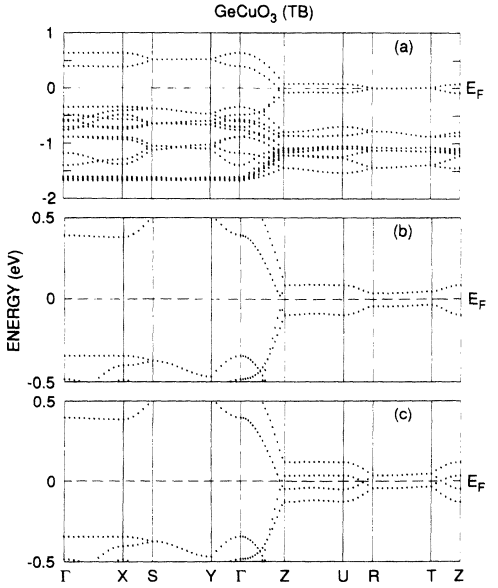

FIG. 6. Comparison between(a) the folded $GeCuO_3$ TB energy bands near E_F for a undistorted nonprimitive cell (i.e., one that is doubled along c) with those involving dimerized Cu's with vertical displacements in neighboring chains that are either (b) antiparallel or (c) parallel.

pected to involve a dimerization within the CuO_2 chains that doubles the unit-cell dimension along c, we plot in Fig. 6(a) the appropriately folded $GeCuO_3$ TB bands near E_F. The flat, fourfold-degenerate bands along the RT line that are pinned at E_F provide a clear signature of an electronic instability in this system. Indeed, a small gap at E_F is opened in Fig. 6(b) when the Cu's in neighboring chains are displaced vertically ($\delta \approx 0.05$ Å) with opposite phases.[14] However, when the Cu displacements in neighboring chains have the same phase, band crossings remain and a zero-gap semiconductor is produced [Fig. 6(c)]. Thus, the present analysis of $GeCuO_3$ favors a staggered pairing of Cu's along neighboring CuO_2 chains and predicts a basic structural feature of the low-temperature spin-Peierls distortion in this system.

To summarize, the results of LAPW band calculations for the spin-Peierls cuprate $GeCuO_3$ yield a pair of unexpectedly narrow ($\sim$ 1 eV) one-dimensional σ^* conduction bands that originate from the edge-sharing feature of the CuO_2 chains in this system. A TB analysis shows that a semiconductor gap can occur within this σ^* band when the Cu dimerization in neighboring CuO_2 chains is staggered. It is expected that charge transport in these σ^* bands will be inhibited (at any level of filling) by the need for intinerant carriers to tunnel through nodal charge-density regions along the chains. Finally, this LDA treatment identifies and provides the basic ingredients (five-band model, TB parameters) for future studies of electron-correlation effects in this system.

Note added in proof. In a recent publication, Nishi has reported neutron-diffraction results on the spin-Peierls transition in $GeCuO_3$ [M. Nishi, J. Phys. Condens. Matter **6**, L19 (1994)] that confirm the present LDA-derived band-structure prediction that the dimerization along the two Cu chains in the cell is out of phase by π.

I am pleased to acknowledge informative conversations with several colleagues on the subject of this investigation, especially S-W. Cheong, S. N. Coppersmith, D. R. Hamann, D. A. Huse, A. P. Ramirez, and T. Siegrist.

[1] M. Hase, I. Terasaki, and K. Uchinokura, Phys. Rev. Lett. **70**, 3651 (1993).
[2] I. S. Jacobs *et al.*, Phys. Rev. B **14**, 3036 (1976).
[3] M. Hase, I. Terasaki, Y. Sasigo, K. Uchinokura, and H. Obara, Phys. Rev. Lett. **71**, 4059 (1994).
[4] G. A. Petrakovskii *et al.*, Zh. Eksp. Teor. Fiz. **98**, 1382 (1990) [Sov. Phys. JETP **71**, 772 (1990)].
[5] T. Hashemi, J. Illingsworth, and A. W. Brinkman, J. Mater. Sci. Lett. **11**, 255 (1992).
[6] H. Völlenkle, A. Wittmann, and H. Nowotny, Monatsh. Chem. **98**, 1352 (1967).
[7] P. Hohenberg and W. Kohn, Phys. Rev. **136**, B864 (1964); W. Kohn and L. J. Sham, *ibid.* **140**, A1133 (1965).
[8] L. F. Mattheiss and D. R. Hamann, Phys. Rev. B **33**, 823 (1986).
[9] O. K. Andersen, Phys. Rev. B **12**, 3060 (1975).
[10] E. Wigner, Phys. Rev. **46**, 1002 (1934).
[11] L. F. Mattheiss and D. R. Hamann, Phys. Rev. B **39**, 4780 (1989).
[12] A. Tauber and J. A. Kohn, Am. Mineral. **50**, 13 (1965).
[13] J. C. Slater and G. F. Koster, Phys. Rev. **94** 1498 (1954).
[14] Approximate Cu-O(2) TB interactions for these distortions are estimated by interpolating linearly the $(pd\sigma)$ and $(pd\pi)$ parameters in Table I.

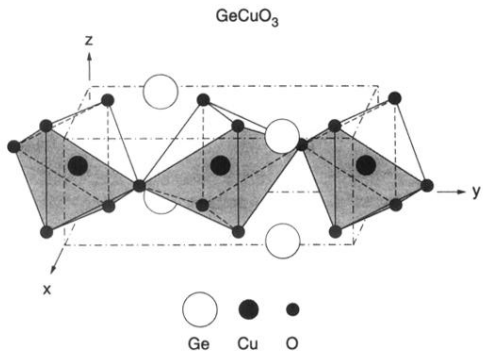

FIG. 1. Primitive orthorhombic cell for $GeCuO_3$ which features a pair of vertex-linked CuO_6 octahedra that share edges along c to form symmetry-related CuO_2 chains with Ge spacers.